Polymer 52 (2011) 1725–1730

Contents lists available at ScienceDirect

Polymer

journal homepage: www.elsevier.com/locate/polymer

High conductivity PEDOT resulting from glycol/oxidant complex and glycol/polymer intercalation during vacuum vapour phase polymerisation

Manrico Fabretto [a,b,*], Carlos Jariego-Moncunill [b], Jussi-Petteri Autere [b], Andrew Michelmore [b], Robert D. Short [b], Peter Murphy [b]

[a] Ian Wark Research Institute, University of South Australia, Mawson Lakes, SA 5095, Australia
[b] Mawson Institute, University of South Australia, Mawson Lakes, SA 5095, Australia

ARTICLE INFO

Article history:
Received 4 November 2010
Received in revised form
21 January 2011
Accepted 18 February 2011
Available online 24 February 2011

Keywords:
Poly(3,4-ethylenedioxythiophene) (PEDOT)
Vacuum-vapour phase polymerisation (V-VPP)
High conductivity

ABSTRACT

Vacuum vapour phase polymerisation (V-VPP) was used to synthesis high conductivity poly(3,4-ethylenedioxythiophene) (PEDOT) on glycol/oxidant coated substrates. Thermo gravimetric analysis (TGA) indicated that up to 15 wt.-% glycol was able to complex with the $Fe(Tos)_3$ oxidant solution and that this loading produced PEDOT with the highest conductivity, namely 1487 S cm^{-1}. Further addition beyond 15 wt.-% resulted in an unbounded excess of glycol which appeared to inhibit the polymerisation process, resulting in reduced doping levels and conductivity. XPS data showed that glycol was incorporated within the PEDOT matrix after polymer synthesis, and that this may contribute to the high conductivity achieved using the V-VPP technique. XPS data also confirmed that the highest conductivity coincided with the highest recorded doping level, $d = 28.4\%$.

1. Introduction

Poly(3,4-ethylenedioxythiophene) (PEDOT) is arguably one of the most highly conductive and stable inherently conducting polymers (ICPs) synthesised to date [1–4]. This has seen PEDOT become one of the most studied ICPs in the open literature, and resulted in a plethora of applications such as; optical displays [5,6], photovoltaic devices [7], organic transistors (OFETs) [8,9], light emitting diodes (OLEDs) [10], and bio-sensing [11]. The ability to alter the band gap structure of PEDOT (and its derivatives) with the addition of pendant groups allows the electronic and optical properties of the polymer to be tailored, further increasing the versatility of this polymer [12,13]. Processing and applying PEDOT onto donor substrates to form devices has, however, been a challenging problem as the polymer is insoluble in aqueous solutions due to its stiff conjugated aromatic backbone structure. To overcome this problem polyanions such as poly(styrene sulfonate) (PSS) have successfully been used to make stable aqueous dispersions of PEDOT [14,15]. Such dispersions are then able to be deposited as thin films onto substrates by way of spin, dip or spray coating *etc*. Dispersions containing PSS have, however, been shown to produce films where PEDOT is encapsulated by the insulating polyanion [16]. Additionally, the films may form alternating PEDOT and insulating polyanion layers [17]. Both these factors contribute to a reduction in the overall conductivity and performance of the deposited films. In an attempt to recoup the decrease in conductivity as a result of using PSS, so called secondary dopants (SDs) [18,19] and organic solvents [20,21] have been used post polymer synthesis. Alternate, *in-situ* synthesis methods have also been developed in an attempt to eliminate the use of PSS all together.

The two most common alternate *in-situ* synthesis methods are electro-polymerisation [22,23] and vapour phase polymerisation (VPP) [24,25]. The former method involves inserting two electrodes into a cell containing a solution of monomer and electrolyte, and a periodic voltage is cycled across the electrodes. Each cycle simultaneously polymerises and deposits the monomer onto the electrode surface. The method does have limitations however, as the polymer can only be formed on conducting substrates and large deposition areas can suffer from lack of film uniformity due to non-uniform electric fields and edge effects. Synthesising conducting polymers using the VPP technique dates back to the mid 1980s with the work of Mohamadi et al. [26], but only recently has the technique gained wide spread acceptance [27–29]. This process is currently producing some of the highest reported conductivity for PEDOT films [2,24,30]. The *in-situ* process involves coating the substrate with an oxidant such as Fe(III) Tosylate ($Fe(Tos)_3$). This is one of the more most common oxidants [31–33], although other oxidants such

* Corresponding author. Ian Wark Research Institute, University of South Australia, Mawson Lakes, SA 5095, Australia. Tel.: +61 8 83023675; fax: +61 8 8302 3683.
E-mail address: rick.fabretto@unisa.edu.au (M. Fabretto).

0032-3861/$ – see front matter © 2011 Elsevier Ltd. All rights reserved.
doi:10.1016/j.polymer.2011.02.028

as $FeCl_3$ [34], $CuCl_2$ [35] and $HAuCl_4$ [36] have been used. In the case of $Fe(Tos)_3$, the Fe salt performs the function of oxidising agent; with the ligand then incorporated as the doping counter ion. The oxidant coated substrate is then placed into a reaction chamber and an EDOT monomer vapour introduced. Condensation of the monomer onto the oxidant coated substrate initiates the polymerisation process, creating a conducting film typically within 30 min.

Many previous VPP studies [37–39] using Fe salts have incorporated weak bases such as imidazole and pyridine to raise the pH of the oxidant. As the base evaporates from the oxidant, a more controlled polymerisation is initiated. Too low a pH has been linked to acidic side reactions during the polymerisation process which deleteriously affects the PEDOT chains [25,39,40]. Controlling the evaporation rate of these weak bases during the VPP process has, however, made their use problematic; even more so with vacuum VPP [41,42]. Levermore et al. [42] produced PEDOT where the conductivity steadily reduced with increasing film thickness. He reasoned that if the base could be replenished during the course of polymerisation it may have been possible to achieve higher conductivity for thicker films. Ha et al. [43] put forward the idea that the weak base imidazole not only reduced the polymerisation kinetics by way of raising the pH of the oxidant $Fe(Tos)_3$, but that it also displaced the hydration water by coordinating with the oxidant. This conclusion was reached by examining both a change in the potentials during cyclic voltammograms and a spectroscopic shift in the absorption peak with increasing imidazole concentration. Recently Fabretto et al. [44] introduced a glycol based surfactant into the oxidant in lieu of weak bases which was shown to moderate the polymerisation rate. Additionally, it did not suffer from the aforementioned evaporation problems during the course of polymerisation. The purpose of this paper is to further elucidate the manner in which the glycol surfactant: i) interacts with the oxidant solution; ii) its role during the polymerisation process and; iii) its function within the PEDOT matrix after polymerisation.

2. Experimental section

Fe(III) Tosylate ($Fe(Tos)_3$) was received from H. C. Starck as a 40 wt.-% solution in butanol (Baytron CB 40). 3,4-ethylenedioxythiophene (EDOT) monomer and the tri-block polymer poly(ethylene glycol-propylene glycol-ethylene glycol) (PEG-PPG-PEG, referred to as 'glycol'), $Mw = 2900$ Da were obtained from Aldrich. All chemicals were used as received.

PEDOT samples were synthesised on 5 × 5 cm glass substrates. The substrates were washed using a mild detergent, followed by an ethanol and high purity water rinse. Prior to spinning the oxidant the substrates were air plasma treated (PDC-32G, Harrick Inc.) for 2 min. The 40 wt.-% $Fe(Tos)_3$ solution was further diluted with butanol to produce a 16 wt.-% solution. Glycol in the weight range 0–50 wt.-% was then added to the oxidant solution. The solution was spin-coated (400B-6NPP, Laurell Technologies Inc.) at a speed of 1900 RPM for 15 s and placed on a 70 °C hotplate for 2 min to evaporate the butanol which produced oxidant layers in the range 6–10 μm. Samples were removed from the hotplate and immediately placed into a 115 L vacuum chamber oven (Binder, Germany) set to 35 °C. The chamber was pumped down to 45 mbar and the internally mounted knife valve and externally mounted bleed valve were opened allowing ingress of EDOT monomer and water vapour respectively. Samples were removed after 25 min and placed on a 70 °C hotplate for 2 min to anneal the polymer (Note: this prevents stress fracturing during the ethanol bath rinse). The sample was then carefully rinsed in an ethanol bath to remove spent oxidant, unbound surfactant, and residual un-reacted monomer. Samples were then placed into an oven at 70 °C for 30 min to remove any solvent.

Elemental analysis of PEDOT films was performed using XPS (SPECS, SAGE, Phoibos 150-HSA) fitted with a non-monochromated Al anode, power 200 W, with a base pressure of 2×10^{-8} mbar. The samples were mounted on the stage and the polymer film was earthed to minimise charging effects. Take off angle was 90° with an incident beam angle of 45°. Sampling depth was approximately 10 nm. Curve fitting was performed with CasaXPS (Neil Fairley, UK) using a linear background. Spectra were charged corrected relative to the aliphatic carbon peak at 285 eV. Full width half maximum (FWHM) for all O1s core line peaks was set to ≈1.9 eV for high resolution spectra, at 20 eV pass energy. Shake up peak FWHM was not constrained. Lineshape was 30% Lorentzian, 70% Gaussian (no tail function required).

Thermal gravimetric analysis (TGA) (TA Instruments, 2950) was performed at a scan rate of 10 °C/min with no lid fitted to the sample pan. Resistivity, R, (Ω/per square) was measured using a four-point probe (RM3, Jandel Engineering), tip radius 100 μm, 60 g preset load and measurements were taken at room temperature (22 ± 2 °C) and humidity (35% ± 5%). Results are the average of at least nine measurements. AFM images and measurements (NTEGRA, NT-MDT) were performed in tapping mode. To measure film thickness, t, (cm) the polymer was carefully scored using a soft scalpel and line scans performed across the groove. Reported thickness is the average of 10 line scans. PEDOT conductivity, σ, (S cm^{-1}) is given by;

$$\sigma = 1/(R \times t) \quad (1)$$

3. Results and discussion

3.1. Glycol-oxidant complex

Our previous work [44,45] using glycols and VPP had indicated that it was a viable alternative to weak bases such as imidazole or pyridine, and its use also overcame the volatility issues with these bases; making it a perfect candidate for use in vacuum VPP. Additionally, quartz crystal microbalance results indicated that glycol also moderated the polymerisation kinetics during VPP. This action had the effect of reducing the apparent reactivity of the oxidant. What was unknown at the time was whether the reduction in apparent activity was the result of the surfactant acting as a simple steric hindrance barrier, or whether the surfactant/oxidant formed a complex which in turn altered the process.

Fig. 1A shows the thermal gravimetric analysis (TGA) of the glycol surfactant, namely weight loss and derivative weight loss. Weight loss is used to identify the relative quantity and different

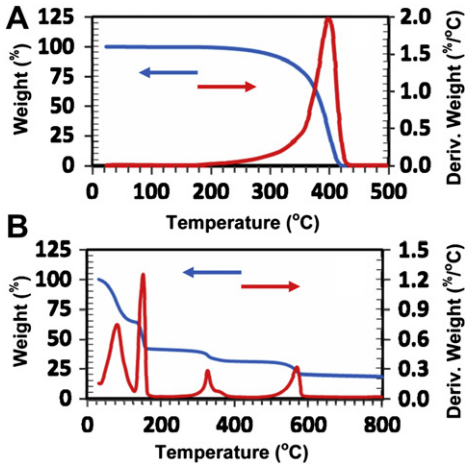

Fig. 1. A) TGA of glycol surfactant and; B) $Fe(Tos)_3$ oxidant.

components present. The derivative weight loss is used to accurately identify at what temperature the majority of that weight loss occurs. The peak weight loss (derivative curve) for glycol is located at 400 °C and only one component is present. Fig. 1B shows the weight loss curves for $Fe(Tos)_3$ without the addition of glycol, and no weight loss peak is present at *ca.* 400 °C. The large decomposition peak located at *ca.* 85–90 °C is trapped solvent evaporating from the oxidant layer (this peak is also present in Fig. 2A–C).

Surfactant in the range 5–50 wt.-% was added to the oxidant solution and TGA was performed (Fig. 2A–C show 15, 25 and 50 wt.-% surfactant addition, respectively). If the addition of glycol surfactant produced nothing more than a surfactant/oxidant mixture then one would rightly expect to see a peak weight loss derivative located at *ca.* 400 °C, regardless of the amount of surfactant added. No peak located at *ca.* 400 °C was evident up to and including 15 wt.-% surfactant addition (Fig. 2A). This result suggests that some physical and or chemical interaction of the surfactant/oxidant has occurred. At a loading of 20–25 wt.-%, a small decomposition peak was evident at *ca.* 420 °C (Fig. 2B), and this peak became progressively bigger and moved towards *ca.* 400 °C as the surfactant was increased up to 50 wt.-% (Fig. 2C). Our interpretation of this result is that up to a loading of 15 wt.-%, all of the available surfactant complexes with the $Fe(Tos)_3$ oxidant. Thus, no weight loss is recorded at *ca.* 400 °C (see Figs. 1B and 2A) until 20 wt-%. Increasing the surfactant addition beyond 15 wt.-% produces a situation where an *unbounded excess* now exists within the oxidant solution, and results in the appearance of a decomposition peak initially located at *ca.* 420 °C. As previously stated, this peak progressively moves towards *ca.* 400 °C as amount of surfactant is increased. The result reaffirms earlier work with respect to surfactant addition, and supports our view that the major contributing factor involved in the decreased polymerisation kinetics is due to the surfactant complexing with the $Fe(Tos)_3$. Thus the inherent steric hindrance of the glycol, in addition to the formation of a surfactant/oxidant complex, has resulted in the oxidant having a reduced apparent reactivity.

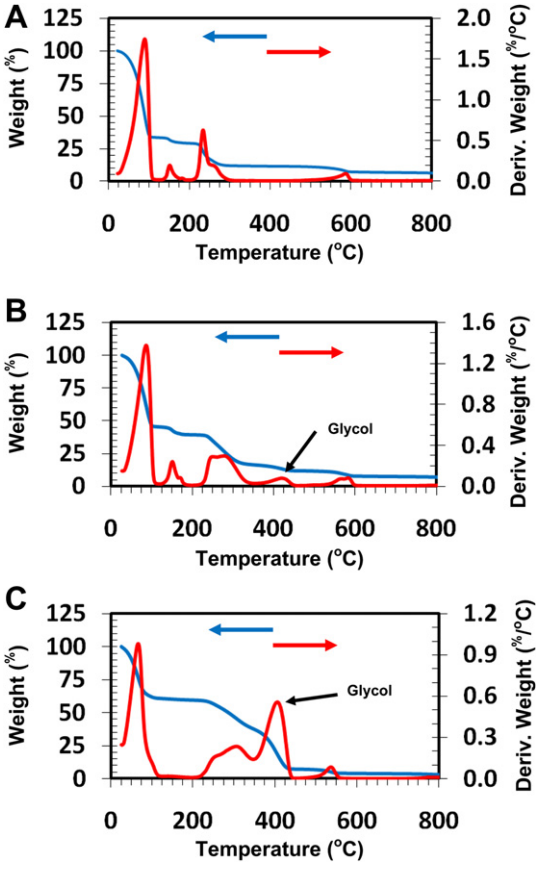

Fig. 2. TGA of glycol in $Fe(Tos)_3$ oxidant. A) 15 wt.-% glycol in oxidant, no glycol peak present; B) 25 wt.-% glycol in oxidant, small glycol peak present at *ca.* 420 °C and; C) 50 wt.-% glycol in oxidant, large glycol peak present at *ca.* 400 °C.

Interestingly, maximum PEDOT film conductivity was also obtained at a 15 wt.-% surfactant loading, with loadings either side of this value resulting in reduced conductivity (see Fig. 3). Presumably, at glycol loadings less than 15 wt.-%, not all of the Fe $(Tos)_3$ is complexed with the surfactant (an inferred result based on Figs. 1 and 2). The most likely outcome would be conjugation defects along the PEDOT backbone. As Fig. 3 shows, at surfactant loadings greater than 15 wt.-% the conductivity progressively falls away. There are two plausible possible reasons for the decrease in conductivity: the increased level of surfactant inhibits the polymerisation process in some manner or; the increased level of surfactant results in a more insulative PEDOT matrix as glycol content is progressively increased. As will be discussed in the next section, the first possibility appears to be the most likely scenario.

3.2. Glycol-PEDOT intercalation

Fig. 3 shows the PEDOT conductivity and film thickness as a function of wt.-% glycol surfactant added to the $Fe(Tos)_3$ oxidant solution. The results are the average of three individual polymerisation runs with a relative error of less than ±5% between the individual runs. At the minimum surfactant loading of 5 wt.-% the conductivity was 436 S cm^{-1} and this increased markedly to form a plateau between 10 and 17.5 wt.-% surfactant addition, with the maximum conductivity of 1487 S cm^{-1} recorded at a loading of 15 wt.-%. Film thickness was initially 73 nm at the lowest surfactant addition and this reduced to *ca.* 66 nm for all but the highest surfactant addition which recorded a thickness of 53 nm. The initial drop in film thickness can be explained in terms of there being less total available oxidant on the substrate as the amount of surfactant is increased. The film thickness, however, remained reasonably constant at 66 ± 1 nm from 10 to 25 wt.-% glycol addition before finally dropping to 53 nm at the highest loading. As the total amount of oxidant available on the substrate decreases with increasing surfactant addition, one would have reasonably expected a concomitant steady reduction in PEDOT film thickness. Excluding the extreme result at a surfactant loading of 30 wt.-%, the reduction in film thickness was about 7 nm and remained reasonably constant over a large range. Such a result strongly points to the possibility that (some of) the surfactant was being incorporated into the PEDOT matrix during polymerisation.

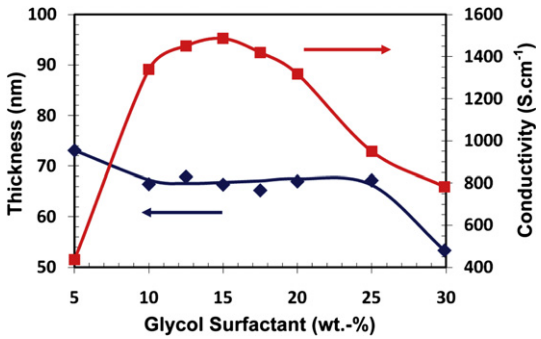

Fig. 3. PEDOT film thickness and conductivity versus glycol surfactant wt.-% in $Fe(Tos)_3$ oxidant solution.

Dkhissi et al. [46,47] theoretically investigated the interplay between PEDOT chains, the counter-ion *p*-toluene sulphonic acid (*p*-TSA) and a small glycol solvent, namely diethylene glycol (DEG). One modelling approach was *implicit* [46]. In this model the "medium" that exists between PEDOT and the counter-ions is assigned the dielectric constant for the DEG solvent, namely $\epsilon = 32$, as opposed to a dielectric constant for vacuum $\epsilon = 1$. This approach although valid is simplistic in that it assumes that the DEG solvent exists throughout the entire polymer matrix. Not surprisingly, inter-molecular distances decreased, and the idea that the solvent would lead to improved ordering and increased conductivity was put forward. Furthermore, the study highlighted the fact that the counter-ion localised the charge distribution along the PEDOT chain (*i.e.* charge pinning). An *explicit* modelling approach [47] was then considered where the DEG molecule was introduced as a "real" solvent. Thus electrostatic screening was localised to the domains occupied by the solvent itself, rather than ubiquitously throughout the polymer matrix. Three different physical locations within the PEDOT matrix were examined for the DEG solvent. For both the *implicit* and *explicit* modelling approaches it was suggested that the solvent might lead to improved ordering of the PEDOT structure, as well as providing some level of charge screening. With this in mind XPS O1s spectra were obtained for PEDOT samples made with surfactant ranging from 0 to 30 wt.-% to quantify the amount of glycol (if any) incorporated within the PEDOT. The same XPS spectra were also used to quantify the different doping levels present in the polymer by measuring the ratios of the areas under the $PEDOT^{(+)}$ and PEDOT curves. Reference O1s spectra for $Fe(Tos)_3$ and the glycol surfactant were obtained prior to measuring the PEDOT films to accurately establish peak locations. Fig. 4 shows the de-convolution of the O1s peaks for the various oxygen species for 0 and 15 wt.-% surfactant addition respectively. The peaks in Fig. 4A (0 wt.-% surfactant) are: tosylate counter $ion^{(-)}$ 531.1 eV; PEDOT 533.2 eV; $PEDOT^{(+)}$ 534.6 eV [48,49]. Although it is generally accepted that the charge along the polymer chain is delocalised, the two de-convoluted peaks, namely PEDOT 533.2 eV and $PEDOT^{(+)}$ 534.6 eV indicate a level of charge "pinning" exits. This observation is consistent with the results of Dkhissi et al. [50] which showed an increased charge density distribution in the vicinity of the counter ion (*i.e.* charge pinning). The broad π to π^* shake up peak is caused by ejected core line electrons colliding with the shared electrons in the π orbital of the ring structure, and is located at 535.7 eV. This π to π^* shake up peak assignment is in agreement with results by Beamson and Briggs for poly(ether sulphone) [51]. In comparison, the de-convolution of the O1s spectra in Fig. 4B (15 wt.-% surfactant) generated an additional peak located at 532.8 eV which has been assigned to the oxygen present in glycol (PEG-PPG-PEG) [51].

XPS is primarily a surface analysis technique having a penetration depth of about 10 nm, with the PEDOT films produced in this study being of the order of 60–70 nm thick. Thus XPS result are only analysing the top 15% of the sample. On the assumption that the XPS measurements are representative of the entire film thickness, Fig. 5 shows the relative quantity of glycol intercalated within the PEDOT matrix. The results are based on the areas under the curves for the XPS spectra of O1s species for different surfactant loadings (relative error $< 10\%$, see also Fig. 4B). The amount of surfactant within the PEDOT matrix progressively increases from zero up until it reaches a plateau at *ca.* 15 wt.-% surfactant addition in the oxidant solution. Interestingly the beginning of the plateau corresponds to both the maximum amount of complexed (or bound) surfactant/oxidant (see Fig. 2) and the point at which maximum conductivity is achieved. Further increases in the amount of surfactant present in the oxidant did not result in additional transfer of surfactant into the PEDOT film. From this, one can deduce that the excess surfactant is rinsed out during the ethanol washing process.

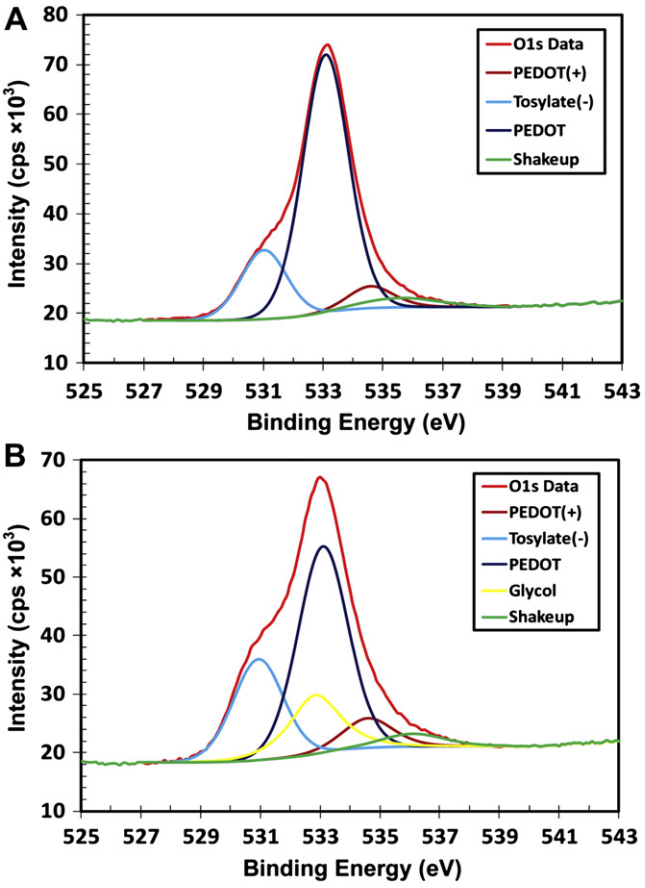

Fig. 4. XPS O1s spectra for PEDOT films synthesised with: A) no glycol surfactant and; B) with 15 wt.-% glycol addition. Peak assignments are: $tosylate^{(-)}$ counter-ion 531.1 eV; PEDOT 533.2 eV; $PEDOT^{(+)}$ 534.6 eV; glycol 532.8 eV and; a broad π to π^* shake up peak 535.7 eV.

So how does one reconcile the conductivity results presented in Fig. 3 with the maximum bound level of surfactant present in the oxidant (TGA results Fig. 2) and subsequently seen in the PEDOT polymer matrix (XPS results Fig. 4)? The ability of the surfactant to moderate the polymerisation rate has already been established in previous worked conducted by Murphy and co-workers [45]. The slowest polymerisation rate was shown to produce the highest conductivity with, presumably, less conjugation defects occurring

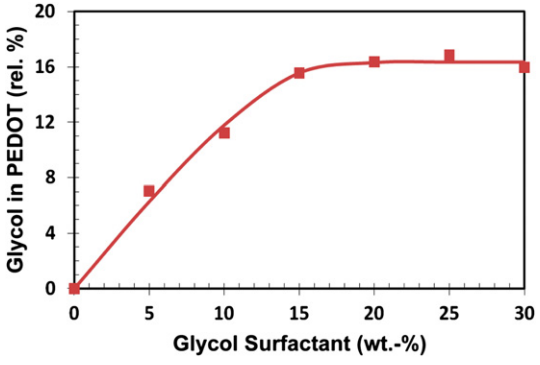

Fig. 5. Relative percentage of glycol content within the PEDOT polymer matrix versus glycol surfactant (wt.-%) in $Fe(Tos)_3$ oxidant solution.

during polymer synthesis. This new study now shows that the apparent reduction in reactivity is largely the result of the surfactant complexing with the oxidant, and that a loading of 15 wt.-% represents the maximum amount of surfactant that can be bound to the oxidant (refer Fig. 2). Beyond 15 wt.-% the increase in the peak at *ca.* 400 °C corresponds to an increase in the amount of unbound surfactant. The conductivity in Fig. 3 shows a steady increase, followed by a plateau, and then a decline as glycol addition is increased. An explanation for the increase in conductivity appears straight forward for reasons already outlined. The decline in conductivity at higher surfactant loadings, however, appears less obvious. Glycol has a relatively high dielectric constant ($\epsilon \approx 32$), therefore it would be reasonable to suggest that as the amount of glycol in the glycol/oxidant was increased, the ensuing increase in glycol within the PEDOT matrix would produce the resulting decrease in conductivity. One cannot, however, argue that this situation is the dominate cause for the decrease in conductivity at high glycol/oxidant loadings. Fig. 5 indicates that glycol incorporation within the PEDOT matrix reaches a plateau at about 15 wt.-% glycol in oxidant and this remains constant up to 30 wt.-%, yet conductivity decreases rapidly after *ca.* 17.5 wt.-% glycol in oxidant addition. A more plausible reason for the decline in conductivity would appear to be that as the surfactant content is increased beyond the amount necessary for all of the $Fe(Tos)_3$ to become bound (complexed), the unbound excess appears to have a disruptive effect during polymer synthesis. Whether this disruption results in point defects along the conjugated backbone and/or a decrease in doping levels will now be examined.

The maximum doping level, *d*, for PEDOT is generally accepted as one dopant anion for every three monomer units (*i.e.* 0.33 or 33%) [15,52,53]. The historical basis for accepting this maximum doping level seems somewhat less than convincing and, in the author's opinion, therefore still open to debate. In one example the basis for accepting 33% as the maximum doping level possible was a "private communication" [54]. Tracing another reference for PEDOT doping [55] lead to two early papers describing reaction conditions for the polymerisation of polypyrrole (PPy) (the assumption, presumably, being that PPy and PEDOT behave in a similar manner) [56,57]. Based on some sound reasoning and experimental data relating to PPy yield versus oxidant concentration, Armes [57] obtained a doping level of $d = 33\% \pm 4\%$, which was later extrapolated to PEDOT synthesis. It is also known that PEDOT undergoes a geometric distortion, changing from an aromatic (benzoid) to quinoid form, during doping [39,50]. As such, perhaps the energetic and physical penalty in doing so, does indeed cap the doping limit to *ca.* 33%. Notwithstanding these concerns, Table 1 reports the doping level, *d*, and conductivity, σ, obtained in this study as a function of wt.-% surfactant addition (*i.e.* glycol/oxidant wt.-%). The maximum conductivity of 1487 S cm^{-1} coincides with the maximum doping level recorded, namely $d = 28.4\%$, at a surfactant addition of 15 wt-%. Further increases in surfactant beyond 15 wt.-% resulted in the doping level falling to $d = 22.8\%$ at the highest loading of 30 wt.-%. Interestingly, however, is the fact that the doping level of $d = 22.8\%$ recorded at 30 wt.-% surfactant was lower than the doping level $d = 25.5\%$ recorded at 5 wt.-% surfactant, yet the conductivity was significantly higher at 783 S cm^{-1} compared to 436 S cm^{-1}, respectively. Such a result indicates that the conductivity of PEDOT, and presumably other conducting polymers, is not just a function of the doping level within the polymer. Conjugation defects along the polymer backbone (and conjugation length) may also play a significant role in determining the overall conductivity. We speculatively put forward that at 5 wt.-% surfactant addition the conjugation along the polymer backbone is compromised during synthesis, with some defects present, but not to the point where doping levels are significantly affected. Contrasting this, at 30 wt.-% surfactant addition the doping level is lower yet conductivity is almost double that recorded at 5 wt.-%. Such a result infers that the conjugated backbone has significantly less defects (an/or increased conjugation length), and that the doping of the polymer has been hindered in some manner. Such a conclusion is consistent with the notion that the excess surfactant present in the oxidant acts as a steric hindrance barrier to counter-ion migration during polymer synthesis. The manner in which the glycol and counter ion are transported and incorporated within the PEDOT matrix is presently not well understood, and is the subject of further investigation.

Table 1
The doping level, *d*, and conductivity, σ, of the PEDOT film as a function of wt.-% surfactant addition into the oxidant solution (*i.e.* glycol/oxidant wt.-%). (Note: doping level, *d*, calculated from the ratio of tosylate$^{(-)}$ to PEDOT plus PEDOT$^{(+)}$ O1s species.)

Glycol Surfactant (wt.-%)	Doping Level (%)	Conductivity (S cm^{-1})
0	16.4	135
5	25.5	436
10	28.0	1339
15	28.4	1487
20	27.9	1318
25	26.7	950
30	22.8	783

4. Conclusions

The addition of the surfactant PEG-PPG-PEG into the $Fe(Tos)_3$ solution has been shown to be a viable alternative to the use of weak bases such as pyridine and imidazole in reducing the apparent reactivity of the oxidant. Results indicate that the surfactant forms a complex with the $Fe(Tos)_3$ oxidant and thus does not suffer from problems associated with volatility, as do the aforementioned weak bases. This makes their use in the V-VPP process far more suitable, from a control viewpoint, during the synthesis process. In comparison the use of weak bases relies on their volatility to trigger the onset of synthesis and finely controlling this process has been shown to be problematic. High levels of glycol addition result in unbound surfactant (*i.e. ca.* >15 wt.-%) being present in the oxidant solution, and a reduction in PEDOT conductivity. At 30 wt.-% surfactant addition the conductivity is almost double that recorded at 5 wt.-%, yet the doping level is lower. This result tends to support the concept of a disruption to the doping process at high glycol addition rather than poor conjugation along the polymer backbone as the major contributing factor. At low surfactant addition (*i.e.* 0 and 5 wt.-%) poor conjugation and doping contribute to reduced conductivity. XPS results indicate that the surfactant forms part of the PEDOT matrix during polymer synthesis. Maximum PEDOT conductivity of 1487 S cm^{-1} coincided with: i) the point at which all of the available oxidant was complexed (bound) with the added surfactant; ii) the maximum recorded doping level of, $d = 28.4\%$ and; iii) the onset of the surfactant plateau within the PEDOT matrix. Excess surfactant in the oxidant solution did not result in additional surfactant being incorporated within the PEDOT matrix, indicating the possibility that the surfactant and counter-ions were incorporated within the PEDOT as an associated pair during polymer synthesis.

Acknowledgements

The authors would like to thank Dr. R. Lazzaroni from the Universite de Mons in Belgium for the many fruitful discussions regarding theoretical aspects of PEDOT doping and structure.

References

[1] Winther-Jensen B, West K. Reactive & Functional Polymers 2006;66:479–83.
[2] Winther-Jensen B, Krebs F. Solar Energy Materials and Solar Cells 2006;90:123–32.
[3] Nardes A, Kemerink M, de Kok MM, Vinkin E, Maturova K, Janssen R. Organic Electronics 2008;9:727–34.
[4] Ouyang J, Chu C-W, Chen F-C, Xu Q, Yang Y. Advanced Functional Materials 2005;15(2):203–8.
[5] Pozo-Gonzalo C, Mecerreyes D, Pomposo J, Salsamendi M, Marcilla R, Grande H, et al. Solar Energy Materials and Solar Cells 2008;92:101–6.
[6] Kang J-H, Oh Y-J, Paek S-M, Hwang S-J, Choy J-H. Solar Energy Materials and Solar Cells 2009;93:2040–4.
[7] Zhang F, Johansson M, Andersson MR, Hummelen JC, Inganas O. Advanced Materials 2002;14(9):662–5.
[8] Wu W, Liu Y, Wang Y, Xi H, Gao X, Di C, et al. Advanced Functional Materials 2008;18:810–5.
[9] Senthilkumar N, Kang H, Park D, Choe Y. Journal of Macromolecular Science Part A-Pure and Applied Chemistry 2010;47:484–90.
[10] Nguyen TP, Le Rendu P, Long PD, De Vos SA. Surface & Coatings and Technology 2004;180–181:646–9.
[11] Bernards D, Macaya D, Nikolou M, DeFranco J, Takamatsu S, Malliaras G. Journal of Materials Chemistry 2007;18:116–20.
[12] Amb C, Beaujuge P, Reynolds JR. Advanced Materials 2010;22:724–8.
[13] Walczak RM, Cowart Jr JS, Abboud KA, Reynolds JR. Chemical Communications; 2006:1604–6.
[14] Jonas F, Heywang G, Schmidtberg W, Heinze J, Dietrich M. Polythiophenes: process for their preparation and their use. US: Bayer AG Germany; 1990.
[15] Kirchmeyer S, Reuter K. Journal of Materials Chemistry 2005;15:2077–88.
[16] Timpanaro S, Kemerink M, Touwslager FJ, De Kok MM, Schrader S. Chemical Physics Letters 2004;394:339–43.
[17] Ionescu-Zanetti C, Mechler A, Carter S, Lal R. Advanced Materials 2004;16(5):385–9.
[18] Martin BD, Nikolay N, Pollack SK, Saprigin A, Shashidhar R, Zhang F, et al. Synthetic Metals 2004;142:187–93.
[19] Ghosh S, Inganas O. Synthetic Metals 2001;121:1321–2.
[20] Ouyang J, Xu Q, Chu C-W, Yang Y, Li G, Shinar J. Polymer 2004;45:8443–50.
[21] Kim JY, Jung JH, Lee DE, Joo J. Synthetic Metals 2002;126:311–6.
[22] Schweiss R, Lubben J, Johannsmann D, Knoll W. Electrochimica Acta 2005;50:2849–56.
[23] Cho S, Xiao R, Lee S. Nanotechnology 2007;18:1–5.
[24] Subramanian P, Clark N, Winther-Jensen B, MacFarlane DR, Spiccia L. Australian Journal of Chemistry 2009;62:133–9.
[25] Winther-Jensen B, Chen J, West K, Wallace GG. Macromolecules 2004;37:5930–5.
[26] Mohammadi A, Hasan M, Liedberg B, Lundstrom I, Salaneck W. Synthetic Metals 1986;14:189–97.
[27] Kim J, Sohn D, Sung Y-E, Kim E-R. Synthetic Metals 2003;132:309–13.
[28] Truong T, Kim D-O, Lee Y, Lee T-W, Park J, Pu L, et al. Thin Solid Films 2008;516(18):6020–7.
[29] Im S, Gleason K. Macromolecules 2007;40:6552–6.
[30] Fabretto M, Zuber K, Hall C, Murphy P, Griesser H. Journal of Materials Chemistry 2009;19:7871–8.
[31] Winther-Jensen B. Base inhibited oxidative polymerisation of thiophenes and anilines with iron (III) salts. International Winther-Jensen B, 2005. p. 1–32.
[32] Zuber K, Fabretto M, Hall C, Murphy P. Macromolecular Rapid Communications 2008;29:1503–8.
[33] Kim TY, Park CM, Kim JE, Suh KS. Synthetic Metals 2005;149:169–74.
[34] Ali M, Kim H, Lee C, Soh H, Lee J. Metals and Materials International 2009;15(6):977–81.
[35] Cho M, Kim S, Nam J, Lee Y. Synthetic Metals 2008;158:865–9.
[36] Cho S, Nam M, Lee J, Youngkwan L. Journal of Nanoscience and Nanotechnology 2008;8(9):4714–7.
[37] Winther-Jensen B, Breiby DW, West K. Synthetic Metals 2005;152:1–4.
[38] Choi J, Yim J, Kim D, Jeon J, Ko Y, Kim Y. Synthetic Metals 2009;159:2506–11.
[39] Lock J, Im S, Gleason K. Macromolecules 2006;39:5326–9.
[40] Winther-Jensen B, West K. Macromolecules 2004;37:4538–43.
[41] Laforgue A, Robitaille L. Macromolecules 2010;43:4194–200.
[42] Levermore P, Chen L, Wang X, Das R, Bradley D. Advanced Materials 2007;13:2379–85.
[43] Ha Y-H, Nikolov N, Pollack SK, Mastrangelo J, Martin BD, Shashidhar R. Advanced Functional Materials 2004;14(6):615–22.
[44] Fabretto M, Muller M, Zuber K, Murphy P. Macromolecular Rapid Communications 2009;30:1846–51.
[45] Fabretto M, Muller M, Hall C, Murphy P, Short R, Griesser H. Polymer 2010;51:1737–43.
[46] Dkhissi A, Beljonne D, Lazzaroni R. Synthetic Metals 2009;159:546–9.
[47] Dkhissi A, Beljonne D, Lazzaroni R, Louwet F, Groenendaal L. Theoretical Chemistry Accounts 2008;119:305–12.
[48] Greczynski G, Kugler T, Salaneck WR. Thin Solid Films 1999;354:129–35.
[49] Wang T, Qi Y, Xu J, Hu X, Chen P. Applied Surface Science 2005;250:188–94.
[50] Dkhissi A, Beljonne D, Lazzaroni R, Louwet F, Groenendaal L, Bredas JL. International Journal of Quantum Chemistry 2003;91:517–23.
[51] Beamson G, Briggs D. High resolution XPS of organic polymers: the Scienta ESCA300 database. John Wiley & Sons; 1992.
[52] Khan M, Armes S, Perruchot C, Ouamara H, Chehimi M, Sj G, et al. Langmuir 2000;16:4171–9.
[53] Im S, Gleason K. Applied Physics Letters 2007;90(15):21121–211213.
[54] Lu J, Pinto NJ, MacDiarmid AG. Journal of Applied Physics 2002;92(10):6033–8.
[55] Corradi R, Armes S. Synthetic Metals 1997;84:453–4.
[56] Armes S, Gottesfeld S, Beery J, Garzon F, Agnew S. Polymer 1991;32(13):2325–30.
[57] Armes S. Synthetic Metals 1987;20:365–71.